1-15-2015

The Terrestrial Uranium Isotope Cycle

Morten B. Andersen

Tim Elliott

Heye Freymuth

Kenneth W.W. Sims

Yaoling Niu

See next page for additional authors

Citation/Publisher Attribution

Andersen MB, Elliott T, Freymuth H, Sims KW, Niu Y, Kelley KA. (2015). "The terrestrial uranium isotope cycle." Nature. 517(7534): 356-9.
Available at: https://doi.org/10.1038/nature14062

The terrestrial U isotope cycle

Morten B. Andersen[1,2], Tim Elliott[1], Heye Freymuth[1], Kenneth W. W. Sims[3], Yaoling Niu[4], Katherine Kelley[5]

[1]Bristol Isotope Group, School of Earth Sciences, University of Bristol, U.K., [2]Institute of Geochemistry and Petrology, Department of Earth Sciences, ETH Zurich, Switzerland, [3]Department of Geology and Geophysics, University of Wyoming, U.S.A., [4]Department of Earth Sciences, Durham University, U.K., [5]Graduate School of Oceanography, University of Rhode Island, U.S.A.

Changing conditions on the Earth's surface can have a remarkable influence on the composition of its overwhelmingly more massive interior. The global distribution of U is a notable example. In early Earth history, U is enriched in the continental crust. Yet after the initial rise in atmospheric oxygen, at ~2.4 Ga, the aqueous mobility of oxidised U results in its significant transport to the oceans and ultimately, via subduction, back to the mantle[1-8]. Here we explore the isotopic characteristics of this global U cycle. We show that the subducted flux of U is isotopically distinct, with high $^{238}U/^{235}U$, as a result of alteration processes at the bottom of an oxic ocean. We further document that mid-ocean ridge basalts (MORB) have $^{238}U/^{235}U$ higher than bulk Earth, confirming the widespread pollution of the upper mantle with this recycled U. Whilst many ocean island basalts (OIB) are argued to contain a recycled component[9], their U isotopic compositions are unperturbed from bulk Earth. Since subducted U was likely isotopically unfractionated prior to full oceanic oxidation at ~600 Ma, this observation reflects the greater antiquity of the OIB source. In detail, elemental and isotope systematics of U in OIB are strikingly consistent with previous OIB Pb model ages[10], indicating formation of these mantle reservoirs between 2.5-1.8

Ga. In contrast, the U isotopic composition of MORB requires convective stirring of recycled U throughout the upper mantle within 600 Ma.

'Recycling' of U from the surface to the Earth's deep interior can be monitored by a decrease in the Th/U ratio of the mantle[2-8]. Thorium provides a valuable reference for several reasons. Firstly, U and Th behave similarly as tetravalent species in the mantle, such that they are difficult to fractionate significantly by melting processes. Only under more oxidised surface conditions do the elements show contrasting behaviour, with Th remaining tetravalent and immobile during weathering, unlike highly water-soluble hexavalent U species. Secondly, both Th and U are refractory, lithophile elements and so the Th/U of the silicate Earth can be estimated from measurements of meteorites. This planetary Th/U reference has recently been refined[11] to a value of 3.876. The Th/U of the terrestrial upper mantle, as inferred from analyses of MORB, is notably lower than this value; two global studies of MORB yield a mean Th/U ~3.1[12,13]. The low Th/U of the upper mantle is attractively explained by addition of significant recycled U from the surface and can be reconciled with a surprisingly high time-integrated Th/U[14], as gauged from $^{208}Pb/^{206}Pb$ ratios, if the U recycling commenced in the latter half of Earth history[2-8]. This makes good geological sense, as prior to the Great Oxidation Event (GOE) at ~2.4 Ga (e.g. see ref. 15) a reduced atmosphere inhibited the surface mobility of U and prevented U recycling.

Here, we test and extend this model of global U cycling using isotopic measurements of U to complement the inferences from elemental Th/U. Recent work[16,17] has shown that surface processes induce U isotopic variations (~1‰) significantly greater than

typical analytical precision (~0.05‰). Natural variations in $^{238}U/^{235}U$ are chiefly linked to the reduction of U(VI) to U(IV) and the magnitudes of such fractionations are inversely proportional to temperature[18,19]. So whilst U isotopic ratios can be perturbed at the surface, the high temperatures and dominance of tetravalent U in the mantle inhibit significant isotopic fractionations at depth. Any "exotic" $^{238}U/^{235}U$ signatures, produced by low-temperature fractionation and transported into the mantle, should therefore provide a robust tracer of surface-processed U.

To explore this potential, we have characterized, to high precision, the $\delta^{238}U$ (the parts per thousand difference in $^{238}U/^{235}U$ relative to a reference solution standard, CRM 145) of a range of samples including: meteorites, mantle-derived basalts and the inputs and outputs of an archetypal subduction zone. A summary of our results is plotted in Fig 1 and reported in Table 1. Measurement precision varied with sample size but for most samples the error on $\delta^{238}U$ was $<\pm 0.03$‰ (2 S.E.). For most samples, resolution of natural variability was limited by our long-term reproducibility. This was gauged from repeat measurements of the geological standard BHVO-2, which yielded $\delta^{238}U = -0.314\pm0.028$‰ (2 S.D. on 21 replicates). We additionally obtained $^{234}U/^{238}U$ measurements, which provide a valuable monitor of recent U disturbance. All key samples gave values within error (±3‰) of secular equilibrium. Further details of analytical procedures and values for a wider range of standards measured are provided in the "methods".

Primitive, chondritic meteorites are typically used as a reference for bulk planetary compositions and so we analysed several ordinary chondrites to try to define a reference 'bulk Earth' $\delta^{238}U$. The very low U contents of chondrites make high-

precision measurements especially challenging, so we further analysed two eucrites. These higher [U] samples should still provide a useful planetary datum given the incompatible, lithophile and refractory nature of U. Our meteorite analyses have $\delta^{238}U$ that range from -0.44‰ to -0.30‰, overlapping with two existing, lower precision determinations of chondritic $\delta^{238}U$ (-0.42±0.09‰[20] and -0.37±0.09‰[21]). The variability in $\delta^{238}U$ of our meteorite analyses, however, is greater than measurement precision and likely reflects recent disturbance of some of our samples (see methods for further discussion). Thus, we propose a planetary estimate based on the weighted average of the two unaltered samples, with ($^{234}U/^{238}U$) within error of unity. This yields $\delta^{238}U$ = -0.306±0.026‰.

We wish to compare the $\delta^{238}U$ of the terrestrial mantle to this new meteoritic datum, inferred to represent 'bulk Earth'. To this end, we have analysed a wide range of basalts (see methods for details), which effectively sample the mantle for an incompatible element such as U. Whilst the shallow convecting mantle is probed by MORB, ocean island basalts (OIB) are widely assumed to be generated from hot, upwelling plumes (possibly containing components from recycled plates) that provide a window into the deeper mantle. We have analysed fresh MORB glass from all three, major oceanic basins and OIB that cover a large portion of mantle heterogeneity as gauged from radiogenic isotopic compositions. It is clear from Fig 1 and Table 1 that MORB and OIB have different mean $\delta^{238}U$. OIB with a wide range of Th/U have $\delta^{238}U$ within error of bulk Earth, whereas MORB have significantly higher $\delta^{238}U$ at lower Th/U. The strikingly super-chondritc $\delta^{238}U$ we observe in MORB would strongly support the scenario of widespread pollution of the upper mantle with surface

U, if recycled U were isotopically heavy. Thus, we examine the U isotopic composition of the subducting plate.

Although variations of $\delta^{238}U$ in the sedimentary environment are now established, appropriate measurements to characterise subducted materials are unavailable. We principally focus on determining the isotopic composition of U added by submarine alteration to the igneous oceanic crust, which is the key flux in accounting for the low Th/U of MORB[6,8]. Comprehensive studies of cores obtained from deep drilling through oceanic crust[8,22,23] demonstrate that heterogeneous addition of U has occurred throughout the upper ~500 m of the altered, mafic oceanic crust (AOC), see also review in ref. 24. Subduction of this 'excess' U is sufficient to lower the Th/U of the upper mantle to 2.5 in ~2 Ga[6].

We have analysed "composite" samples from ODP Site 801, which penetrates 420 m into ~170 Ma Pacific mafic crust[25]. The composites are mixtures of the different lithologies and alteration styles present, blended as powders in representative proportions. This is an efficient means of obtaining a reliable average composition of the heterogeneously altered mafic crust[22,25]. The $\delta^{238}U$ of the composites vary from -0.45‰ in the uppermost part (0-110 m) to higher values (-0.15 to +0.16‰) in the deeper part (110-420 m) see Table 1. This variability likely reflects a change from oxic incorporation of U near the surface[26] to (partial) reductive U roll front type sequestration[27] in keeping with a general observed change in alteration style[8,25]. The "super-composite" from Site 801, representing a weighted average of the full 420 m upper crustal section has $\delta^{238}U$ = -0.17‰ and [U]= 0.39 μg/g, 5 times higher than the unaltered basalts[8]. This super-chondritic value for the average $\delta^{238}U$ reflects the

dominance of reductive addition of U(IV) to the upper oceanic crust as a whole (see methods for further information). Interestingly, MORB compositions lie close to a simplistic mixing line between this average altered crustal composition and the "bulk Earth" reference (Fig 1).

Finally we assess the consequences of subduction for the U isotope composition of recycled crust, using the Mariana arc as a well understood example. During subduction, material is lost from the down-going plate and incorporated into magmas erupted at island arcs. The Mariana arc lavas show evidence for two slab-derived components; a melt from the sedimentary section and a 'fluid' from the mafic oceanic crust[28]. A regression line through the array of Marianas lavas in Fig 1 should point towards the sediment component at high Th/U and the fluid component at low Th/U. The average $\delta^{238}U$ of sediments subducting beneath the Mariana (-0.35±0.04‰, Table 1) is compatible with the compositions of the lavas with high Th/U whilst an extension of the array of Mariana arc lavas to low Th/U indicates that the 'fluid' derived from the mafic oceanic crust has a low $\delta^{238}U$. Such an isotopically light composition can be explained if either the U is preferentially lost from the uppermost altered mafic crust (see Fig 1), or else if U isotopes are fractionated during (partial) loss from the plate. In either case, the U that is lost to the arc is isotopically lighter than the bulk input to the subduction zone and so U transported beyond the arc must become even heavier than its initial composition.

Thus, we are confident that modern surface cycling of U results in a substantial flux of isotopically heavy U into the mantle. This observation provides a ready explanation for the super-chondritic $\delta^{238}U$ of MORB. The isotopically heavy U must

be carried in the altered, mafic crust beyond the zone of arc magmatism but subsequently lost to the upper mantle (Fig 2). Transport of U in an accessory mineral such as allanite[29] is a possible means to effect this outcome.

Like MORB, many OIB have significantly sub-chondritic Th/U, indicative of the addition of recycled U to their sources. Yet all OIB have $\delta^{238}U$ in error of "bulk Earth", which is inconsistent with the modern U-cycle. We noted above, however, that the high $\delta^{238}U$ characteristic of average recent oceanic crust is the result of partial reduction of U-rich, oxidised seawater as it percolates through the submarine volcanic edifice. This scenario has only been possible in the last ~600 Ma, since the second rise in oxygen in the late Proterozoic and the establishment of fully oxic oceans (e.g. see ref. 15). Between 600 Ma and the initial rise of oxygen at ~2.4 Ga, U was mobile during surface weathering but rapidly scavenged from the reduced oceans[15]. Quantitative removal of riverine U supplied to the oceans would result in a flux of U to the sea-floor that was isotopically unfractionated (see Fig 2 and methods). The implications of this conceptual model are that OIB sources formed from recycled oceanic crust between 2.4 Ga and 0.6 Ga should have increasingly sub-chondritic Th/U, but chondritic $\delta^{238}U$. Furthermore, any OIB source formed earlier than 2.4 Ga should have both chondritic Th/U and $\delta^{238}U$.

We have further investigated this idea using Pb model ages of several OIB suites. Their Pb model ages are calculated according to a 2-stage model, similar to that of Chase (10), see methods for details. As with Chase (10), we find that OIB have a range of source model ages. Notably these ages correlate with the Th/U of the samples (Fig 3), in the manner discussed above. We show two plots in Fig 3: one

with time-integrated Th/U as determined from Pb isotopes (Fig 3a) and the other with measured Th/U (Fig 3b). Not unsurprisingly, the data using time-integrated Th/U form a tighter array, since any recent Th/U fractionations from source composition during melting and melt migration to the surface are removed (see methods for detailed discussion). However, both plots independently document a similar relationship with Th/U becoming increasingly sub-chondritic in OIB sources younger than ~2.4 Ga.

The remarkable implication of the ideas presented above is that the two-stage rise in atmospheric oxygen, reconstructed from observations on the Earth's surface, is reflected in the Th-U-Pb systematics of mantle-derived basalts. The coherence of our observations with those anticipated from a first order model of U-recycling also lends credence to the significance of Pb model ages of OIB sources[10]. The range of OIB model ages therefore place valuable constraints on the maximum and minimum incubation times of an OIB reservoir, potentially the residence time of subducted slabs at the base of the mantle before becoming sufficiently buoyant to return to the surface. Furthermore, our inference that isotopically heavy U has only been introduced into the mantle over the last 600 Ma places a maximum timescale for its effective stirring into the MORB source. This value is reassuringly consistent with an estimate based on a markedly different approach using Pb isotopes[30].

References main text

1 Albarède, F. & Michard, A. Transfer of continental Mg, S, O and U to the mantle through hydrothermal alteration of the oceanic crust. *Chemical Geology* **57**, 1-15 (1986).

2 Zartman, R. E. & Haines, S. M. The plumbotectonic model for Pb isotopic systematics among major terrestrial reservoirs—A case for bi-directional transport. *Geochimica et Cosmochimica Acta* **52**, 1327-1339 (1988).

3 McCulloch, M. T. The role of subducted slabs in an evolving earth. *Earth and Planetary Science Letters* **115**, 89-100 (1993)..

4 Kramers, J. D. & Tolstikhin, I. N. Two terrestrial lead isotope paradoxes, forward transport modelling, core formation and the history of the continental crust. *Chemical Geology* **139**, 75-110 (1997)

5 Collerson, K. D. & Kamber, B. S. Evolution of the continents and the atmosphere inferred from Th-U-Nb systematics of the depleted mantle. *Science* **283**, 1519-1522 (1999).

6 Elliott, T., Zindler, A. & Bourdon, B. Exploring the kappa conundrum: the role of recycling in the lead isotope evolution of the mantle. *Earth and Planetary Science Letters* **169**, 129-145 (1999).

7 Zartman, R. E. & Richardson, S. H. Evidence from kimberlitic zircon for a decreasing mantle Th/U since the Archean. *Chemical Geology* **220**, 263-283 (2005).

8 Kelley, K. A., Plank, T., Farr, L., Ludden, J. & Staudigel, H. Subduction cycling of U, Th, and Pb. *Earth and Planetary Science Letters* **234**, 369-383 (2005).

9 White, W. M. and Hofmann, A. W., 1982. Sr and Nd isotope geochemistry of oceanic basalts and mantle evolution. *Nature* **296**, 821-825.

10 Chase, C. G. Oceanic island Pb: two-stage histories and mantle evolution. *Earth and Planetary Science Letters* **52**, 277-284 (1981).

11 Blichert-Toft, J., Zanda, B., Ebel, D. S. & Albarède, F. The Solar System primordial lead. *Earth and Planetary Science Letters* **300**, 152-163 (2010).

12 Gale, A., Dalton, C. A., Langmuir, C. H., Su, Y. & Schilling, J. G. The mean composition of ocean ridge basalts. *Geochemistry, Geophysics, Geosystems* **14**, 489-518 (2013).

13 Jenner, F. E. & O'Neill, H. S. C. Analysis of 60 elements in 616 ocean floor basaltic glasses. *Geochemistry, Geophysics, Geosystems* **13** (2012).

14 Galer, S. J. G. and O'Nions, K., 1985. Residence time of thorium, uranium and lead in the mantle with implications for mantle convection. *Nature* **316**, 778-782.

15 Lyons, T. W., Reinhard, C. T. & Planavsky, N. J. The rise of oxygen in Earth'searly ocean and atmosphere. *Nature* **506**, 307-315 (2014).

16 Stirling, C. H., Andersen, M. B., Potter, E.-K. & Halliday, A. N. Low temperature Isotope Fractionation of uranium. *Earth Planetary Scientific Letters* **264**, 208-225 (2007).

17 Weyer, S. *et al.* Natural Fractionation of 238U/235U. *Geochimica et Cosmochimica Acta* **72**, 345-359 (2008).

18 Fujii, Y., Nomura, M., Onitsuka, H. & Takeda, K. Anomalous isotope fractionation in uranium enrichment process. *Journal of Nuclear Science and Technology* **26**, 1061-1064 (1989).

19 Bigeleisen, J. Temperature dependence of the isotope chemistry of the heavy elements. *Proceedings of the National Academy of Sciences* **93**, 9393-9396 (1996).

20 Connelly, J. N. *et al.* The absolute chronology and thermal processing of solids in the solar protoplanetary disk. *Science* **338**, 651-655 (2012).

21 Goldmann A., Brennecka, G., Noordmann J., Weyer S. & Wadhwa, M. The 238U/235U of the Earth and the Solar System. *Geochimica et Cosmochimica Acta* in press.

22 Staudigel, H., Davies, G. R., Hart, S. R., Marchant, K. M. & Smith, B. M. Large scale isotopic Sr, Nd and O isotopic anatomy of altered oceanic crust: DSDP/ODP sites417/418. *Earth and Planetary Science Letters* **130**, 169-185 (1995).

23 Bach, W., Peucker-Ehrenbrink, B., Hart, S. R. & Blusztajn, J. S. Geochemistry of hydrothermally altered oceanic crust: DSDP/ODP Hole 504B – Implications for seawater-crust exchange budgets and Sr- and Pb-isotopic evolution of the mantle. *Geochemistry, Geophysics, Geosystems* **4**, 8904 (2003).

24 Dunk, R. M., Mills, R. A. & Jenkins, W. J. A reevaluation of the oceanic uranium budget for the Holocene. *Chemical Geology* **190**, 45-67 (2002).

25 Kelley, K. A., Plank, T., Ludden, J. & Staudigel, H. Composition of altered oceanic crust at ODP Sites 801 and 1149. *Geochemistry, Geophysics, Geosystems* **4** (2003).

26 Brennecka, G. A., Wasylenki, L. E., Bargar, J. R., Weyer, S. & Anbar, A. D. Uranium isotope fractionation during adsorption to Mn-oxyhydroxides. *Environmental Science & Technology* **45**, 1370-1375 (2011).

27 Bopp IV, C. J., Lundstrom, C. C., Johnson, T. M. & Glessner, J. J. Variations in 238U/235U in uranium ore deposits: Isotopic signatures of the U reduction process? *Geology* **37**, 611-614 (2009).

28 Elliott, T., Plank, T., Zindler, A., White, W. & Bourdon, B. Element transport from slab to volcanic front at the Mariana arc. *Journal of Geophysical Research: Solid Earth (1978–2012)* **102**, 14991-15019 (1997).

29 Hermann, J. Allanite: thorium and light rare earth element carrier in subducted crust. *Chemical Geology* **192**, 289-306 (2002).

30 Rudge, J. F. Mantle pseudo-isochrons revisited. *Earth and Planetary Science Letters*, **249,** 494-513 (2006).

Supplementary Information is linked to the online version of the paper at www.nature.com/nature.

Acknowledgments. Financial support for this research was provided by NERC grant NE/H023933/1. We thank the Natural History Museum, London, and M. Anand for providing meteorite samples. H. Staudigel & T. Plank were instrumental in producing and curating AOC composite samples. We are grateful to C. Taylor for careful picking of MORB glasses, E. Melekhova for preparing the quenched glass and D. Vance for comments. As ever, C. Coath kept the mass-spectrometers purring.

Author Contributions. Analytical developments were done by M.A. Sample preparation and analyses were carried out by M.A. and H.F. MORB samples and altered ocean crust composites were provided by K.S, Y.N. and K.K. All authors

contributed with discussions. T.E. carried out the Pb-modeling. T.E. and M.A. prepared the manuscript.

Author Information. Data can be found in the EarthChem portal (cp.iedadata.org). Reprints and permissions information is available at www.nature.com/reprints. The authors declare no competing financial interests. Readers are welcome to comment on the online version of the paper. Correspondence and requests for materials should be addressed to morten.andersen@erdw.ethz.ch.

Figure 1 | Uranium isotopic compositions ($\delta^{238}U$) vs. Th/U ratios for mantle-derived basalts and altered oceanic crust. Fig 1a**,** OIB (circles) have $\delta^{238}U$ similar to 'bulk Earth' (crossed square), whereas the higher $\delta^{238}U$ and lower Th/U of MORB (diamonds) imply a mixture (shown as a grey line) between 'bulk Earth' and average modern altered oceanic crust, AOC (square, showing ODP 801 super-composite). Mariana arc basalts (triangles) show positive co-variation of Th/U ratio and $\delta^{238}U$, reflecting mixing of two components: i) a sedimentary source, with high Th/U and $\delta^{238}U$, ii) a low Th/U, low $\delta^{238}U$ similar to the upper section of the AOC (open triangle, showing 0-110 m ODP 801 composite). The brown arrowed line shows a best fit of the Mariana arc data pointing towards the inferred 'fluid' component from the AOC. Fig 1b shows a histogram highlighting the distinctively heavy U isotope composition of MORB relative to bulk Earth and most OIB.

Figure 2 | Cartoon of the terrestrial U isotope cycle over the history of Earth. (top) Prior to the Great Oxidation Event (GOE) at ~2.4 Ga, low atmospheric oxygen levels limited U mobility on the surface. (middle) The GOE would have heralded an enhanced U weathering flux to the oceans. Quantitative release of U during weathering would yield a U flux to the oceans with $\delta^{238}U$ ~-0.3‰, and quantitative extraction of U into the dominant reducing sinks from the ocean, including AOC, would also give a $\delta^{238}U$ of ~-0.3‰ for any 'recycled' U delivered to the mantle. (bottom) During the last 600 Ma U is isotopically fractionated during partial, reductive uptake of U into the AOC from the now largely oxic oceans. This fractionated U in the subducted AOC U flux is released at different depths; initially the isotopically light U in the uppermost crust is lost to arc magmatism, whilst the heavy U from the deeper crust is released beyond the arc front into the convecting

upper mantle. The residual, deep-subducted crust has a U isotopic composition similar to unaltered MORB.

Figure 3 | Pb model ages versus Th/U in OIB mantle sources. 2 stage Pb model ages (^{207}Pb-^{206}Pb ages[29]) versus (a) time-integrated Th/U (using measured ^{208}Pb-^{206}Pb and model source age) and (b) measured Th/U for the same suite of OIB samples; (1) Hawaii; (2) Iceland; (3) Azores I; (4) La Palma; (5) French Polynesia; (6) Samoa; (7) Sao Miguel II; (8) Réunion (see methods for details). Despite potential recent disturbance of the measured Th/U in OIB samples, both plots document a similar relationship of decreasing Th/U with decreasing Pb model ages. These increasingly sub-chondritic Th/U ratios are consistent with progressive U addition into the mantle from subduction since the GOE at ~2.4 Ga.

Table 1 | Summary of δ^{238}U for sample groups

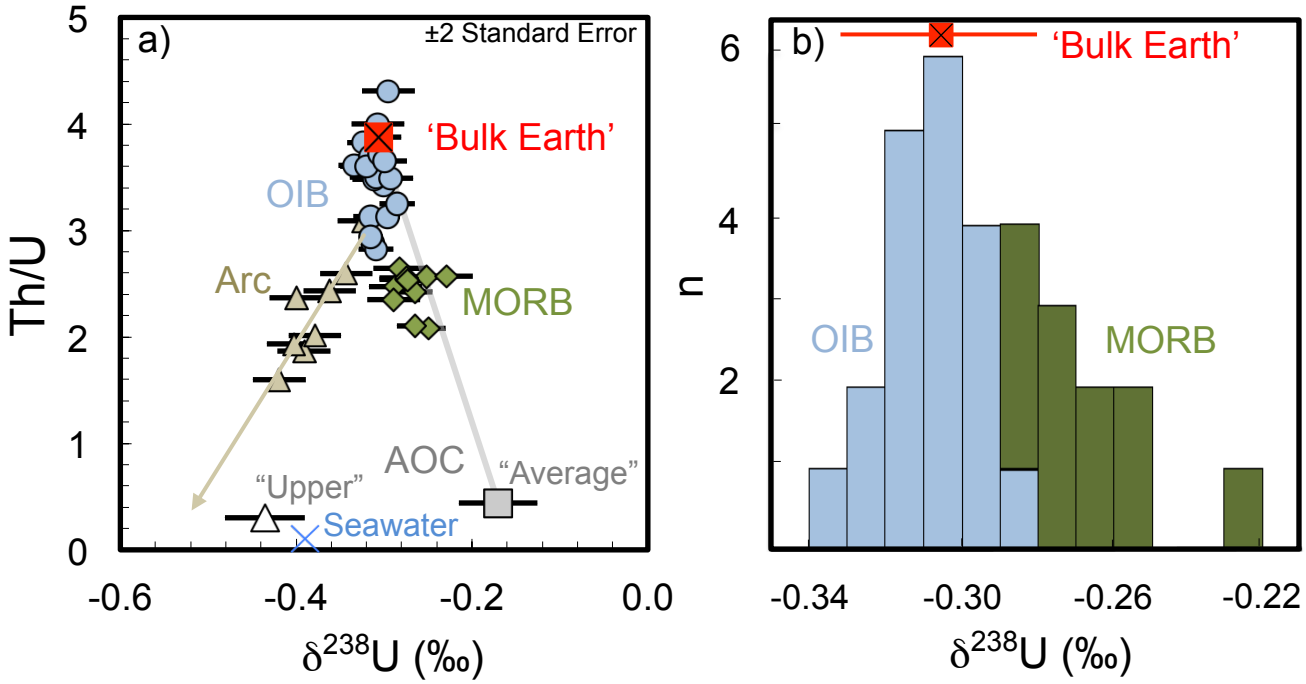
a)
±2 Standard Error
'Bulk Earth'
OIB
Arc
MORB
AOC
"Upper"
"Average"
Seawater
Th/U
δ238U (‰)
b)
'Bulk Earth'
OIB
MORB
n
δ238U (‰)

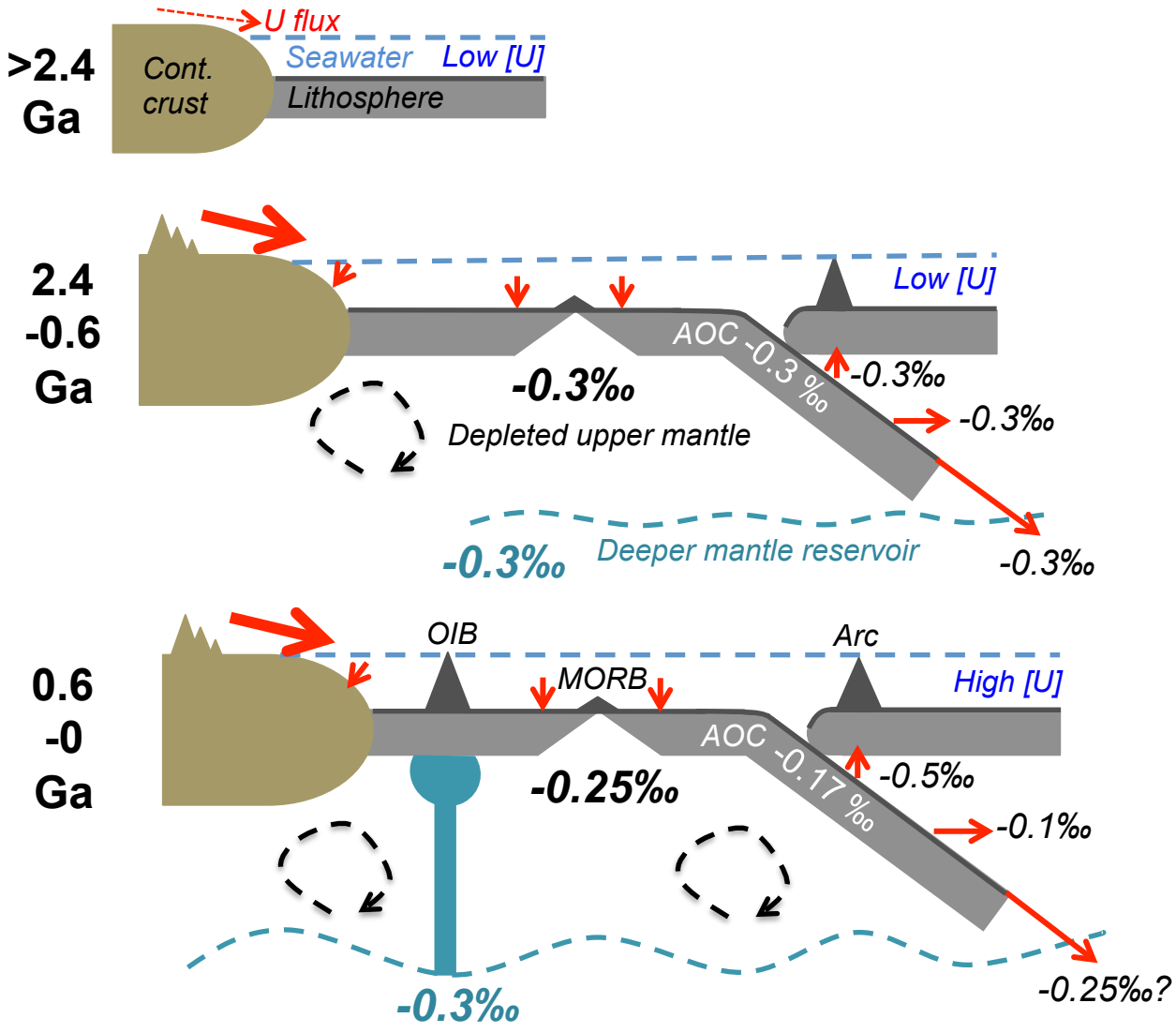
>2.4 Ga
U flux
Cont. crust
Seawater
Low [U]
Lithosphere
2.4 -0.6 Ga
Low [U]
AOC -0.3 ‰
-0.3‰
-0.3‰
-0.3‰
Depleted upper mantle
-0.3‰
Deeper mantle reservoir
-0.3‰
0.6 -0 Ga
OIB
Arc
MORB
High [U]
AOC -0.17 ‰
-0.5‰
-0.25‰
-0.1‰
-0.3‰
-0.25‰?

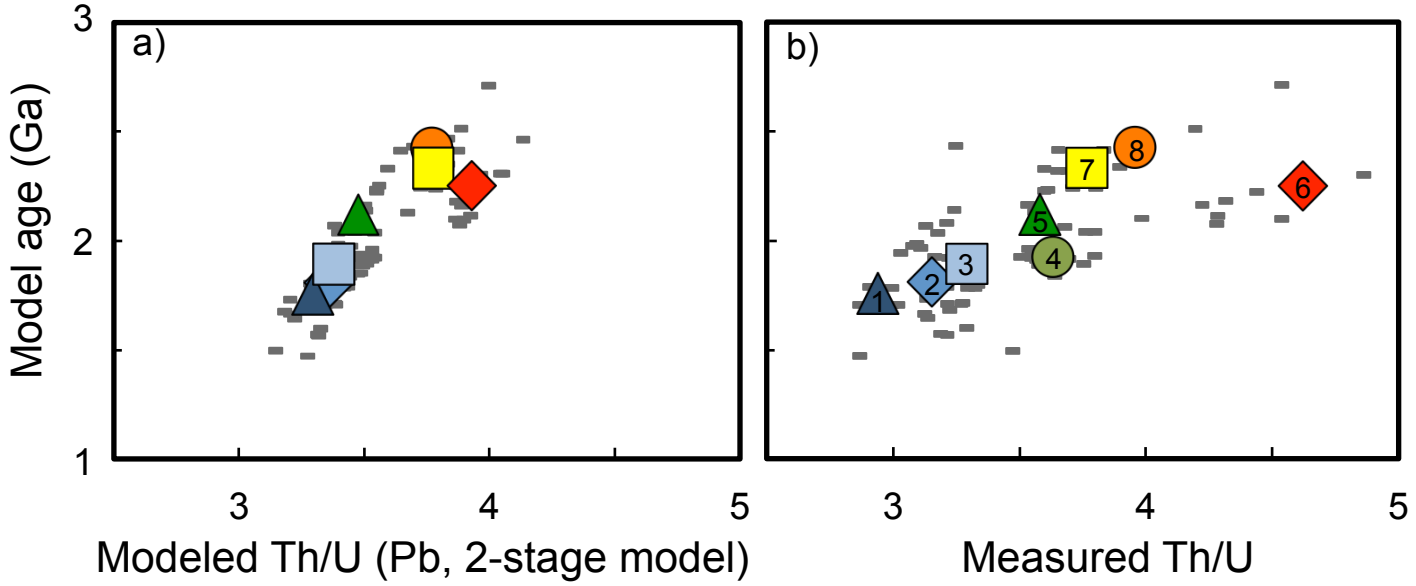
a)
b)
Model age (Ga)
3
2
1
3
4
5
Modeled Th/U (Pb, 2-stage model)
Measured Th/U
1
2
3
4
5
6
7
8

Table 1 | Summary of $\delta^{238}U$ for sample groups*

Samples type	$\delta^{238}U$ ±2SE	Th/U	N.
Unaltered Meteorites ('Bulk Earth')	-0.306 ±0.026	3.84	2
OIB	-0.308 ±0.005	3.48	19
MORB	-0.268 ±0.011	2.44	11
Altered Mafic Oceanic Crust			
Average	-0.170 ±0.026	0.44	1
0-110m	-0.436 ±0.042	0.30	3
110-220m	+0.164±0.086	0.45	3
220-420m	-0.145 ±0.045	0.44	3
Mariana Arc Lavas			
Guguan (fluid rich)	-0.405 ±0.023	1.73	2
Uracas (sediment rich)	-0.333 ±0.016	2.84	2
Average Mariana Sediments	-0.354 ±0.039		7
Seawater (open-ocean)	-0.390 ±0.006		3

**A full table with individual data is presented in Supplementary Data Table 1*

Methods

Sample preparation

With two main exceptions, existing powders of most samples were used. Generally there were prepared and have previously been documented by the authors. Powdered samples of bulk meteorites were prepared at the University of Bristol for this study, from chips carefully picked under the microscope to be free of alteration, fusion crust or signs of saw-mark blades. Likewise, all MORB samples were prepared afresh by picking mm-sized fragments of glass without signs of alteration, surface coatings or devitrification.

Given the low U concentrations of MORB, the consequences of possible secondary U addition by absorption to marine Fe-Mn oxyhydroxide coatings is a concern. Although careful hand-picking should address this problem, we further processed the picked glass, using a mildly reductive procedure based on methods for dissolving Fe-Mn coatings in marine sediments, using a mixture of 0.05 N hydroxylamine hydrochloride – 15% acetic acid – 0.03 Na-EDTA at a pH of ~4 (ref 31). Similar approaches have been used in preparing MORB glasses for U-series analysis[32-34]. Each sample was leached three consecutive times by adding 12 ml of the leaching solution to the bulk samples in pre-cleaned centrifuge tubes, and placing these in a vortex shaker for 24 hours at room temperature. Samples were thoroughly rinsed in 18 MΩcm (hereafter MQ) water following each leaching step.

The elemental concentrations of each leach solution were determined using the Element 2 ICP-MS of the Bristol Isotope Group, using already established methods[35]. Potential contaminant U removed in each leach fraction was monitored using the total

U concentration and ratios of U to immobile elements Th, Sc, Ti and Zr (Supplementary Data Table 2). For most samples, the first leach released U in higher proportions than the immobile elements, however, at the end the three leaching steps the U to refractory element ratios approached the ratios measured in the total bulk (residual) MORB sample after full dissolution. This suggests that any minor, absorbed U was effectively leached away. The U removed during reductive leaching represented only 1 to 4% of the total U that remained in the bulk residue. All MORB samples have ($^{234}U/^{238}U$) within a few permil of secular equilibrium, except D18-1 which had a ($^{234}U/^{238}U$) ~14‰ above secular equilibrium, suggesting that some U contaminant was still present after the reductive leaching. The elevated ($^{234}U/^{238}U$) of seawater (1.146) suggests that this contamination is marine-derived. Despite the minor residual U contamination, we have chosen to leave it in our dataset, but note its value is not as robust as the other measurements (see later for further discussion).

In addition to the natural samples, a basalt powder was made into a glass and leached to assess if the reductive leaching caused any U isotope fractionation in the residual glass. Given the small total amounts of U removed during leaching and that the final leach solutions appeared to have removed material with bulk glass composition (Supplementary Data Table 2), it seemed unlikely that leaching would bias the U isotopic composition of the residue, but for completeness we tested this. A basalt powder was melted in a platinum crucible and subsequently quenched by dropping the platinum crucible into a MQ water bath at room temperature. Given the young ages of the MORB glasses in this study, they have experienced little U-series alpha-recoil damage and can therefore be directly compared to the leaching of the artificial quenched glass. Measurements of the quenched glass gave identical $\delta^{238}U$ before and

after the reductive leaching step (-0.23±0.03 versus -0.24±0.03‰) and ($^{234}U/^{238}U$) (0.995±0.003 and 0.999±0.002) respectively, showing that the leaching process does not fractionate the U isotopes of fresh glass.

Sample dissolution, spiking and column chemistry

Sample sizes up to ~1.5 gram were dissolved in a single beaker. For larger samples (e.g. chondrites and MORB) several splits of the same sample were dissolved separately and then all aliquots were combined after full dissolution. Terrestrial silicates were dissolved in a mixture of conc. HF-HNO_3- $HClO_4$ acid and fluxed on a hotplate for 24 hours and dried by stepwise increasing the temperature from 120° to 200°C. Samples were then fluxed twice in ~6 N HCl (~15 ml per gram of sample) on a hotplate (120°C) and dried down in between. Samples were re-dissolved in 7 N HNO_3 and then diluted down to 2 N HNO_3 for TRU Resin column chemistry. Both the eucrites (~1 gram) and the ordinary chondrites (~4 grams in 3 aliquots) were initially dissolved in a similar way to larger terrestrial silicate samples. However, after the 7 N HNO_3 step the dissolution was incomplete and a residue of dark residue remained. These residues were isolated from the remaining dissolved sample and refluxed in a 3 ml conc. HNO_3 – 1 ml conc. HCl mixture in a high-pressure, Anton-Paar asher (200°C and 100bar pressure, in silica glass vials). This step fully dissolved the residues, which were then remixed with the already dissolved sample aliquots, dried down and redissolved in 7 N HNO_3 prior to TRU Resin chemistry in 2 N HNO_3.

All samples were spiked with the IRMM-3636 ^{233}U-^{236}U double spike[36] (aiming for $^{236}U/^{235}U$ of ~5), either prior to dissolution or prior to column chemistry for combined dissolved sampled with separately processed aliquots.

The U was separated from all other matrixes in a two-step procedure by (1) TRU Resin and (2) UTEVA chemistry. The TRU Resin chemistry was optimized for large sample sizes with ~2 ml resin loaded in polypropylene Bio-Rad columns. Up to ~1 gram of sample were loaded on each column. Samples were loaded and matrix eluted using 40 ml 2 N HNO_3 and U was collected in 8 ml 0.3 N HF–0.1 N HCl. Samples were then dried down and fluxed in conc. HNO_3-H_2O_2 to eliminate any organic material from the resin bleeding into the sample. For large samples that were split over several columns, these were homogenized at the end of this phase and then be dried down to be re-dissolved in 3 N HNO_3 for UTEVA chemistry. The UTEVA chemistry was performed in shrink-fit Teflon columns containing ~0.6 ml of resin. Loading and matrix elution steps used 20 ml of 3N HNO_3, before elution of Th in 3 ml of 3 N HCl, and collection of the purified U in 8 ml 0.3 N HF–0.1 N HCl. Samples were then dried down, fluxed in conc. HNO_3-H_2O_2, dried down and re-dissolved in the requisite amount of 0.2 N HCl for the desired U concentration (100-300 ppb) for MC-ICPMS measurements. Full uranium recovery (>95%) was obtained using this method with total chemistry blanks of <20 pg for all samples (negligible compared to sample sizes >20 ng).

MC-ICPMS Measurement setup

The U isotope measurements were conducted on a Thermo Finnigan Neptune MC-ICP-MS (Serial No. 1002) of the Bristol Isotope Group, University of Bristol, running in low mass resolution (M/ΔM ~500) and using an Aridus desolvating nebulizer introduction system. Uranium sample sizes of 40-150 ng were consumed during individual analysis. The data were collected in static mode in a similar fashion to that

described in Andersen et al. (37). All cups are connected to feedback amplifiers with 10^{11} Ω resistors, except for the ^{238}U cup, which was connected to a feedback amplifier with a 10^{10} Ω resistor to accommodate a larger ion beam. Uranium tailing and hydride formation were monitored as described in Andersen et al. (37). Both the 237.05/^{238}U abundance sensitivity and the hydride and high-side tailing formation at 1 a.m.u. (measured as 239.05/^{238}U) were 2-3 x 10^{-6} and remained stable during each measurement session. The low-mass side tailing contributions to ^{234}U, ^{235}U and ^{236}U were estimated, and corrected for, from interpolation of a linear - log fit to mass versus tailing intensity, as used in Hiess et al. (38). Furthermore corrections for $^{232}ThH^{+}$ and 1 a.m.u. high-mass tailing on ^{233}U were made to measurement, assuming similar behavior for Th and U. These were of minimal importance, however, due to the good separation of U from Th during UTEVA the chemistry (^{232}Th/^{233}U < 1).

Measurements were conducted using typical ion beam intensities of ~1 nA for ^{238}U, ~7 pA for ^{235}U, ~40 pA for ^{236}U and ^{233}U and ~0.05 pA for ^{234}U, integrated over a period of 80 x 4 seconds. Washout and on-peak blank measurements were similar to those described in Andersen et al. (37). On-peak U blank intensity never exceeded 10 ppm of the total ^{238}U beam of the sample and was generally <2 ppm.

The Neptune was equipped with a large plasma interface pump (turbo-booster) offering enhanced transmission efficiency when combined with “jet+X cones”, as opposed to “standard+X cones”. The data obtained are identical for both set-ups (See supplementary Data Tables 3 and 4). General U transmission efficiencies were ~1.5% for “standard+X cones” and ~3% for “jet+X cones”.

After, tailing and hydride corrections, the measured $^{233}U/^{236}U$ ratio was used for mass bias correction, using the exponential mass fractionation law[39]. To obtain $^{234}U/^{238}U$, $^{235}U/^{238}U$ ratios the minute ^{238}U, ^{235}U and ^{234}U contributions from the IRMM-3636 spike were subtracted. Based on a calibration using CRM-145 (Supplementary Data Table 3), the U isotope ratios used for the Bristol IRMM-3636 were: $^{236}U/^{233}U$ = 0.98130, $^{236}U/^{238}U$ = 4259, $^{236}U/^{235}U$ = 21988 and $^{236}U/^{234}U$ = 2770. These ratios are identical to the certified ratios from IRMM-3636 (Ref. 36) for $^{236}U/^{233}U$ (= 0.98130±0.00015), $^{236}U/^{238}U$ (= 4259±7) and $^{236}U/^{235}U$ = 21988±36), but slightly diverge for $^{236}U/^{234}U$ (= 2732±4). Measurements of all unknown samples were bracketed individually and normalised to CRM-145 standard measurements, spiked with IRMM-3636, in a similar fashion to the unknowns.

Measurement performance, reproducibility and accuracy

For each measurement sequence, the mean of the absolute $^{238}U/^{235}U$ of the CRM-145 standard used was typically within ±50 ppm of the value (137.832) reported for the NBL 112a standard[38] and the $^{234}U/^{238}U$ ratios were within ±2‰ of published ratios for the CRM-145 standard[37]. The ($^{234}U/^{238}U$) activity ratios were calculated using the half-lives of Cheng et al. (40). All samples in this study are normalized to CRM-145 standard negating any uncertainty relative to deviations from the absolute ratio for the CRM-145 standard as potentially related to a non-exponential component of instrumental mass fractionation.

Given the use of mixed feedback amplifier resistors with different response times, internal error estimates may give a misleading impression of true precision (e.g. see ref. 41). Thus, to test the full external reproducibilities for individual unknown

samples, a total of eight splits of BHVO-2 were individually processed (dissolution, spiking and chemistry) and measured during different analytical sessions (with different setups, see Supplementary Data Table 4). The external reproducibility of $\delta^{238}U$ for BHVO-2 was ±28 ppm (2 S.D.) and similar or better external reproducibility was obtained for 2 aliquots of the basalt LP 45 E (a historic basanite from La Palma), the in-house CZ-1 uraninite and three open-ocean seawater samples (see Extended Data Item 1). Other samples measured in duplicate agreed within their 2 standard error estimates (See Supplementary Data Table 4). The reproducibilities of $^{234}U/^{238}U$ were limited by the low ^{234}U intensities (<0.2 pA), but were ±3 ‰ or better for the standards.

Potential artifacts on the measured $\delta^{238}U$ from different U/matrix ratios are unlikely given that ordinary chondrites (low U/matrix ratio) and OIB (high U/matrix ratio) both have lower $\delta^{238}U$ compared to MORB (intermediate U/matrix ratio). Furthermore, consistent results are obtained when comparing the standards measured in this study and other studies using comparable normalising standards (NBL 112a[17], SRM-950a[21] and CRM-145[16]). The measured uraninite CZ-1 standard ($\delta^{238}U$ = -0.053±0.029‰) is within error of the value reported in Stirling et al. (ref 16; -0.10±0.07‰). Similarly, the BHVO-2 measurements in this study ($\delta^{238}U$ = -0.314±0.028‰) compare well with measurements in Goldmann et al. (ref 21; -0.32±0.07‰). Finally, our open ocean seawater measurements ($\delta^{238}U$ of -0.390±0.018‰) agree well with open ocean seawater measurements in Weyer et al. (ref 17; -0.41±0.03‰).

Uranium in extraterrestrial material and a bulk Earth $\delta^{238}U$

Previous work has shown large variability in the $\delta^{238}U$ of extraterrestrial material[20,21,42-46]. Thus, even if it exists, estimating a uniform chondritic $\delta^{238}U$ composition is challenging. Some of the observed $\delta^{238}U$ heterogeneity has been attributed to variable addition of ^{235}U from the decay of, now extinct, ^{247}Cm (see ref. 45). However, meteorites also show relative depletions in ^{235}U indicating that other processes may play a role (e.g nucleosynthetic anomalies, planetary formation processes)[20,21,42,46]. Additional concerns are terrestrial perturbation of U, which may be indicated from the physical preservation and anomalous chemical composition. Specifically for U, Th/U departing from the recently defined meteoritic reference[11] and ($^{234}U/^{238}U$) activity ratios out of secular equilibrium, may testify to planetary body processes[47] or terrestrial perturbation.

Due to the generally low U abundance in meteorites, it is necessary to obtain large chondrite samples (~5-10 g) to allow high precision $\delta^{238}U$ measurements, which can run counter to Museum loan policies. Thus we initially honed our technique on 3 large desert meteorite "finds" (M2, M12 and M15), provided by M. Anand from the Open University. These had previously been studied petrographically and characterised at the University of Bristol. We had prepared several hundreds of grams of powder from the interiors of these ordinary chondrites. As "finds", however, these samples were potentially perturbed by terrestrial weathering. We subsequently obtained large (~25 g) samples of two "falls" (Zag and Saratov) from 'meteoritemarket.org'. All these samples are ordinary chondrites, which are not only more readily available than carbonaceous chondrites, but are isotopically more similar to the Earth (e.g. see refs 48,49).

We supplemented our ordinary chondrite measurements with analyses of two eucrites, Juvinas and Stannern, kindly provided by the Natural History Museum, London. Eucrites have higher U contents and so require smaller sample sizes (~1 g) for high precision analyses. Although differentiated meteorites, the isotope ratio of a highly incompatible element such as U should be minimally affected during crust formation and so we believe these samples still provide a valuable planetary reference. Notably eucrites generally have chondritic Th/U ratios[50-52], indicating an absence of elemental fractionation during their formation. The eucrite samples we analysed were "falls" and so likely less prone to terrestrial weathering than the finds.

Of the ordinary chondrites, two gave identical, but relative low $\delta^{238}U$ ratios (M15; -0.439±0.030‰ and Saratov; -0.442±0.050‰) whereas the three others were all within error but ~100 ppm higher (M2; -0.322±0.030‰, M12; -0.326±0.022‰, Zag; -0.301±0.050‰). The eucrites also differed in their $\delta^{238}U$ (Juvinas; -0.312±0.030‰ and Stannern; -0.369±0.030‰) but with Juvinas overlapping with the compositions of the heaviest ordinary chondrites (see Extended Data Item 2).

The three ordinary chondrite desert "finds", have elevated ($^{234}U/^{238}U$) ratios (1 to 12 % ^{234}U excess) suggesting oxidative weathering during their time at the Earth's surface, with oxidation of Fe potentially promoting mineral surfaces for U sorption, with a positive correlation between U concentration and ($^{234}U/^{238}U$) ratios (Extended Data Item 2). Furthermore, Saratov also had ~1% elevated ($^{234}U/^{238}U$), whilst Stannern was ~1% depleted in ($^{234}U/^{238}U$) relative to secular equilibrium. Only the ordinary chondrite "Zag" and eucrite "Juvinas" were at secular equilibrium for ($^{234}U/^{238}U$). The independent constraints provided by ($^{234}U/^{238}U$), show that only

Juvinas and Zag can be considered pristine and notably their $\delta^{238}U$ are within error of each other (Extended Data Item 2).

Perturbation of U in the meteorite samples is also indicated by their Th/U ratios relative to the planetary reference value[11] of 3.876±0.016. The ordinary chondrites with the lowest $\delta^{238}U$ have the highest [U] and lowest Th/U, further suggestive of U addition. Three samples (Juvinas, Zag and M2) have Th/U in error of the reference value and all of these have $\delta^{238}U$ within error of each other (Extended Data Item 2). However, given the minor ($^{234}U/^{238}U$) excess in M2, we do not include this in our best estimate of 'bulk Earth', $\delta^{238}U$ = -0.306±0.026‰, provided by the weighted average and weighted 2 standard error of Juvinas and Zag. Despite demonstrable open-system behavior of U, the mean of all meteorite samples gives a $\delta^{238}U$ of -0.36±0.04‰ (±2 standard error of the mean), which is within error of the weighted estimate from pristine samples (Extended Data Item 2). Although our best estimate of 'Bulk Earth' from our meteoritic samples is only defined by two samples, and would usefully be substantiated by additional measurements, we believe that the systematics of the altered samples provide important evidence to support the significance of this best estimate. Moreover, in terms of our main observations on terrestrial samples the choice is not critical; for either the mean of all the meteorites or just the pristine ones, the $\delta^{238}U$ of MORB are heavier whilst the $\delta^{238}U$ of OIB are unresolved from these meteoritic values.

$\delta^{238}U$ in Ocean Island Basalts

A suite of 19 ocean island basalts from Iceland, Cape Verde, Azores, Canary Islands and Hawaii were measured. Further details on these samples are provided in the

Supplementary Data Table 1. We have dominantly used historic samples, collected previously for U-series studies, which have the major advantage of being fresh. Notably, we analysed 4 non-historic, but still relatively young (~1 Ma) and ostensibly petrographically fresh samples from La Palma, Canary Islands. Two of these samples (LPF 96-39 and CS20) yielded ($^{234}U/^{238}U$) out of equilibrium, chastening us against using older samples from possibly more extreme weathering environments elsewhere. Nevertheless, these two samples showing clear open-system U-series behavior with ($^{234}U/^{238}U$) ~2% lower than secular equilibrium, these are still within error of the other La Palma samples for $\delta^{238}U$ and so we did not exclude these data from our averages. This also indicates that $\delta^{238}U$ is not hugely sensitive to minor perturbations of the U budget.

In terms of traditional radiogenic isotope characterization, the islands we have studied cover high $^{3}He/^{4}He$ (Hawaii, Iceland), HIMU (La Palma, Canaries), EMII (Sao Miguel, Azores) and FOZO (Pico, Azores and Fogo, Cape Verde) 'flavours' of mantle signatures[53-55]. Although La Palma is not as radiogenic in its lead isotope ratios as the classic French Polynesian and St. Helena localities, the latter have suffered ~10 million of years of tropical weathering and so are far from ideal for characterising primary U isotope ratios. We have not measured any representative samples from EMI-type mantle, but nevertheless cover a large compositional range of OIB.

$\delta^{238}U$ in Mid-Ocean Ridge Basalts

We have measured eleven glassy, axial or near axial MORB samples from all three major ocean basins, Indian (n=1), Atlantic (n=3) and Pacific (n=7). Further details on

these samples are given in Supplementary Data Table 1 and associated references[56-60]. All picked glasses were leached to remove possible absorbed U on ferro-manganese coating, as discussed earlier. The eleven MORB glasses have Th/U of 2.1 to 2.6 and all have ($^{234}U/^{238}U$) within a few permil of secular equilibrium, except the already discussed Atlantic Ocean sample D18-1. As for the OIB with perturbed ($^{234}U/^{238}U$), the $\delta^{238}U$ does not appear strongly affected and D18-1 has $\delta^{238}U$ = -0.265±0.030‰, identical to the mean $\delta^{238}U$ of all MORB, so we did not exclude this data point from our averages. This observation is compatible with a mass balance calculation to account for the observed ($^{234}U/^{238}U$) disequilibrium of D18-1 assuming the contaminant is having U isotope compositions similar to seawater. Adding seawater with ($^{234}U/^{238}U$) of 1.146 to MORB at secular equilibrium predicts a change in $\delta^{238}U$ of less than 0.02‰ given a seawater $\delta^{238}U$ of -0.39‰.

$\delta^{238}U$ in Island Arc Volcanics

A suite of nine mafic samples from the Mariana arc front[28] was selected to investigate subduction zone processes (see Supplementary Data Table 1). These well-characterised samples show variable subducted sediment input to their sources combined with a rather constant flux of 'fluid' from the subducting, mafic oceanic crust[28]. In more detail, it has recently been argued that the sediment component evident in the arc lavas is dominated by the volcaniclastic horizons rather than representing an average of all lithologies, in which pelagic clay plays a significant role[28,61]. Samples with small sediment contributions, as marked by high $^{143}Nd/^{144}Nd$ and low Th/Nb, have low Th/U and high ($^{238}U/^{230}Th$), implying a recent, slab-derived U addition to their mantle source. The systematic compositional variations of these lavas allow us to extrapolate towards the possible $\delta^{238}U$ of this slab-derived fluid,

using a best-fit linear regression line through the data in the Th/U vs. $\delta^{238}U$ space, as shown in Fig. 1 in the main text.

$\delta^{238}U$ of subduction zone inputs

Subducted crust can be separated into three principal, chemical components; unaltered oceanic crust, altered mafic oceanic crust (AOC) and sediments. Here we analysed sediments and AOC from well-characterised deep ocean drill holes[8,25,62], ODP 801 and 802 in the west Pacific, to assess the U budget of subduction-related material. Not only does this location provide the best opportunity to assess the mean composition of the old AOC (~170 Myr), but since it is placed in front of the Mariana arc, the composition of the overlying sediments are specifically appropriate as the endmember for the Mariana arc lavas.

Typical assemblages for the deeper ocean sediment package that are subducted, include volcaniclastics, pelagic clays, cherts, carbonates and Fe-Mn crusts. The uranium concentrations for these materials are variable in the 0.1-10 ppm range. Modern seawater has a U concentration of ~3.2 ppb and a homogeneous $\delta^{238}U$ of -0.390±0.010‰ (see Supplementary Data Table 1). Biogenic carbonate appears to incorporate U from seawater without any significant isotope fractionation[63]. The measured deep-sea pelagic clays and volcaniclastics are close to the seawater $\delta^{238}U$ and the bulk Earth value (-0.42 to -0.28‰, Supplementary Data Table 1). Furthermore, the Site 801 composite sample "801SED", meant to reflect an average of the infilling material between the pillow basalts within the basement (comprising of chert, hydrothermal deposit, calcite and clay minerals) has a $\delta^{238}U$ similar to seawater. Thus, the Mariana and indeed most subducting sediment packages have an

average $\delta^{238}U$ close to the values for modern seawater and bulk Earth.

The most important source of "U excess" in subduction zones is the AOC. The fluid-induced alteration in oceanic crust can generally be classified into high-temperature (>100°C) and low-temperature (<100°C) types.

The high-temperature alteration generally occurs close to the spreading ridge axis and at greater depth in the crust by percolation of hot hydrothermal fluids[64,65]. Any seawater-derived U uptake in these settings is assumed to be quantitative (e.g. see ref. 66), however, the deeper sections of the crust (<1000 m) affected by high-temperature hydrothermal circulation are generally little altered and have low U concentrations close to typical MORB (e.g. 0.07 ppm)[65]. Thus, the high-temperature alteration at greater depth does not appear to add a significant amount of U compared to the shallower low-temperature alteration[24].

The low-temperature alteration (<100°C) dominates at ridge-flanks with percolation of less intensely heated seawater[65,67], and the uppermost 500 to 1000 m of the mafic oceanic crust, experiences significant U addition[8,22-25,64] with a mean 5-fold U content relatively to the unaltered mid-ocean ridge basalts[8]. The low-temperature alteration is therefore the area of most uptake of additional U in the subducting plate. Thus we have focussed our attention on characterising this low temperature alteration using average, 'composite' samples (see below).

Altered, mafic oceanic crust

For estimating the U concentration and $\delta^{238}U$ budget of altered oceanic crust, we have

made high precision $\delta^{238}U$ analyses on "composites" from the upper ~500 meters of altered extrusive lavas at the well-studied ODP Site 801. This represents a substantial section of the extrusive lavas erupted at a fast spreading centre[68]. Secondary alteration products from hydrothermal seawater flow-through suggest alteration temperatures from 10-100°C increasing downwards[62]. A typical alteration sequence consists of oxic celadonite formation around alteration veins, followed by Fe-hydroxides and later reducing saponite and pyrite, in a zone moving away from the alteration veins and into the host rock[62]. Carbonate precipitates also occur, which may have formed intermittently through time[8,62]. Uranium enrichments are evident in breccia zones and in relation to redox haloes, with U concentrated at the boundary between oxidized (celadonite-rich) and reduced (saponite/pyrite-rich) zones moving away from the alteration veins, in a roll-front redox type U deposition pattern[8,62]. These redox haloes dominate the deeper part of the drilled section[8,62]. In Kelley et al. (8) it is estimated that about 50% of total U excess is hosted in the secondary formed carbonates and the remaining is associated with the redox haloes.

From the main (tholeiitic) ~420 m alteration zone, three suites of "composite" samples from different depth ranges (0-110 m, 110-220 m, 220-420 m) have been prepared to average the composition of the heterogeneously altered sections in the crust[25]. The composites are physical mixtures of powders in relative proportions of their abundances throughout the particular section of core and intended to physically represent the bulk composition of various depth domains within the drilled sequence. For each of the three composite zones three different powder mixtures were prepared: "FLO" composites represent the least altered material, "VCL" the most altered material and "MORB" composites represent the bulk (mixtures of the FLO and VCL

composites)[25]. Furthermore, a "super-composite", comprising an integration of the full upper 420 meters of core, was made[25]. All the composite samples have low Th/U ratios (0.1-0.6), and high U concentrations of ~0.4 ppm[25]. The U concentration of the 801 super-composite (0.39 ppm) is similar to the DSDP 417/418 super-composite (0.3 ppm) and significantly higher than estimated unaltered MORB (0.05 ppm)[69].

The $\delta^{238}U$ was measured in the three composite sections (in all three "FLO", "VCL" and "MORB" powder mixtures), the super-composite and three individual samples. The $\delta^{238}U$ in the composite samples are variable through the ~420 meter sequence; the upper ~110 meters averages -0.436±0.042‰, the middle ~110 meters are significantly heavier, averaging +0.164±0.086‰ and the lower ~200 meters are in between, averaging -0.145±0.045‰ (see Supplementary Data Table 1). The "super-composite" sample yielded a $\delta^{238}U$ of -0.170±0.026‰. In addition to the composite samples we analysed three single samples from different depths; (1) a capping alkali-basalt (-0.333±0.044‰) from ~26 m above the "start composite depth" of the altered crust section; (2) an altered MORB (-0.341±0.044‰) in the upper composite section (~-100 m) and a calcitic breccia (-0.114±0.044‰) from the lowest composite zone (~-320 m). The differences in $\delta^{238}U$ between the latter two, normal, individual altered oceanic crust samples are reassuringly consistent with the composites, with the shallower sample showing significantly lower $\delta^{238}U$ than the deeper one. The alkali basalt sample has a high U content (0.7 ppm), presumably reflecting its primary composition, which will be much less influenced by secondary U addition than MORB. Alkaline volcanism is atypical of oceanic crust stratigraphy but a feature of some West Pacific drill sites, believed to be part of the burst of plume volcanism in the Cretaceous[25]. Fittingly, this alkali basalt sample has a $\delta^{238}U$ similar to other OIB

(see Supplementary Data Table 1).

The variable $\delta^{238}U$, at values distinct from seawater, shows that the seawater-derived U is not quantitatively incorporated during alteration in the Site 801 AOC. During U uptake involving no redox transition, U isotopes generally appear to yield similar or slightly lower $\delta^{238}U$[16,17,26,63,70]. However, during the U(VI) to U(IV) reduction process U isotope fractionation is governed by both the nuclear field shift and mass-dependent mechanisms[71,72]. These processes lead to U isotope fractionation, but in opposite directions, with the nuclear field shift dominating the total observed $^{238}U/^{235}U$ fractionation and leading to a preference for the heavy isotope in the reduced immobile U(IV) form[18,19,71,72]. Such shifts towards higher $\delta^{238}U$, during redox-driven U uptake, have been documented in natural environments including U-enriched reducing sediments[17,37,63] and redox-driven roll-front U ore deposits[27,73,74]. With mass-balance considerations in mind, it is clear that the U incorporation constitutes a partial reduction process, as a complete reduction of the available U would result in no net isotopic fractionation. This implies a process in which U is partitioned between U(VI) and U(IV) species but only the latter is fixed, and left immobile, with the former being transported away in the percolating fluid. Such a loss of isotopically light U during a partial U reduction process preferentially taking up heavy U isotopes, has been shown in groundwaters associated with roll-front U ore deposits[73], *in-situ* bio-stimulated U reduction flow-through experiments[75] and the anoxic Black Sea water column[76].

For the AOC at Site 801, the $\delta^{238}U$ lower than the seawater composition in the upper 100 meters may be expected from a dominant oxic U uptake, through adsorption,

consistent with relatively oxidised conditions and high water/rock ratios[62]. A change to higher $\delta^{238}U$ in the lower part of the AOC is in accordance with general U addition through a reductive process and U(VI) to U(IV) transition in the deeper part of the AOC with more restricted seawater flow-through[62,64]. Furthermore, the loss of isotopically light U to the upper part of the crust will mean that fluids percolating deeper may anyway have higher $\delta^{238}U$ signatures than the seawater composition. Both the lower and the middle part of the altered mafic crust have $\delta^{238}U$ higher than seawater, with the highest $\delta^{238}U$ found in the middle part. This observation may be related to the basement structure at Site 801, with variable permeability and, hence, through-flow of seawater[62] and, consequently, heterogeneous U addition throughout the AOC. From the deposition of brown oxic haloes throughout the Site 801 AOC, Alt & Teagle (62) estimated that most oxic seawater through-flow occurred in the upper 150 m and below 300 meters depth in the core and, consequently, the most reducing conditions are in between. This may explain why the highest $\delta^{238}U$ is found in the middle part, as U incorporated through U reduction are more dominant in this zone, compared to U uptake from oxic adsorption in the upper and lower sections.

Strikingly, the measured $\delta^{238}U$ and the U concentrations are very similar for the least altered (FLO) and most altered (VCL) material in each of the composite sections. This suggests that it is not the degree of alteration that dictates the U incorporation, but the ambient conditions. The relatively high $\delta^{238}U$ of the super-composite suggests that the reduced U in the deeper part of the AOC dominates the overall $\delta^{238}U$ signature.

Assuming such roll-front redox U uptake, as seen in the AOC 801, is representative of

modern AOC U uptake and represents the integrated modern AOC for subduction, it delivers a high $\delta^{238}U$ to the mantle. In more reduced conditions U is expected to be taken up in a more quantitative manner, resulting in little net isotopic fractionation of the added U. Such a scenario may be expected for the alteration of mafic oceanic crust from the percolation of anoxic seawater which dominated the deeper ocean prior to the second rise in atmospheric oxygen ~600 Ma[15,77]. This scenario would suggest insignificant U isotopic fractionation for U uptake into AOC prior to ~600 Ma, yielding a $\delta^{238}U$ similar to the mean $\delta^{238}U$ composition of rivers, the major U input into the ocean. At present, the best estimate of the modern riverine $\delta^{238}U$ flux to the ocean is -0.24‰[78], close to our bulk Earth estimate. This suggests that U is released near-congruently with little net U isotope fractionation during oxidative terrestrial weathering and riverine transport. Assuming near congruent U release during terrestrial weathering since the great oxidation event ~2.4 Ga, and oxidation of the atmosphere, quantitative uptake of U into the AOC would then imply a $\delta^{238}U$ composition near bulk Earth in the period ~2.4 Ga to ~600 Ma.

Th-U-Pb systematics of OIB

The database: Our simple model of U recycling predicts that samples derived from increasingly young mantle sources will have increasingly sub-chondritic Th/U. To test this prediction we compiled data from the literature for samples, which have been analysed for both Th and U concentrations and Pb isotope compositions (see Extended Data Item 3). The latter provide model age constraints, as detailed below.

In order to minimize the effects of analytical problems and secondary weathering processes obscuring primary signatures, we placed quite selective criteria for inclusion of samples into the dataset, namely:

1. We only included samples with mass-spectrometric, isotope dilution data on Th and U concentrations, coupled with U-series disequilibrium data. This ensures high precision Th/U data and provides additional information on the magnitude of possible perturbation by the melting process (see below). Moreover, since samples collected for U-series data are all young, this also guards against U perturbation during weathering. As discussed above, mobility of U during weathering is otherwise a significant concern.

2. We have only selected data from the main, shielding building phases of islands. Later, post-erosional lavas are frequently invoked to contain a lithospheric component[79,80], which do not reflect the deep source we seek to investigate.

3. In cases where several datasets exist for the sample location, we select the one containing the likely more robust techniques. Thus in the case of the Azores, we use the data from Elliott et al. (81) rather than Turner et al. (82) as the MC-ICPMS Pb data of the former provide much less scattered model ages than those obtained from TIMS measurements of the latter.

Our database (Extended Data Item 3) thus comprises of analyses from Hawaii, Iceland, Canary Islands (La Palma), Azores (Pico and São Miguel), Society Islands and Samoa. We also include a composite data point for Réunion derived from separate U-series and Pb isotope studies of historic eruptions. Although these studies are dominantly on different sample suites, the well-documented, extreme isotopic homogeneity of historic Réunion magmatism[83] gives us confidence to combine the

mean values of Th/U and Pb isotopes. There is one island (Pitcairn) for which appropriate data exists according to our criteria, but which we have not plotted for practical reasons. Namely, the very unradiogenic Pb isotope ratios of this island yields negative model ages in our calculations and so cannot be plotted together with the other data. This combined with their extremely high Th/U suggest that additional processes are responsible for the striking characteristics of this 'EMI' type composition, e.g. erosion of deep continental crust[84]. In all, our compiled OIB database covers a similar wide range of isotopic characteristics as represented by samples analysed for $\delta^{238}U$ (main text Fig. 1) and so forms a fitting complement.

In main text Fig. 3 we plot each individual datum from our compilation as a point, to show the range of compositions. To emphasise the contrasting mean compositions of different islands we have also averaged individual samples from a given island. A comment is required about the averaging of the Azores samples. The island of São Miguel has a marked spatial isotopic heterogeneity, with a distinct geographic (W-E) variation. Thus we have added samples from the western volcanic centre (Sete Cidades) to the Pico samples to represent 'normal' Azores (I) while the other, more easterly samples are averaged to give 'enriched' Azores (II).

Pb model ages: It has long been known that a slope on the plot of $^{206}Pb/^{204}Pb$ vs $^{207}Pb/^{204}Pb$ potentially has age significance (e.g. ref. 85). Chase (10) used this approach to some effect, using the linear arrays in $^{206}Pb/^{204}Pb$ vs $^{207}Pb/^{204}Pb$ defined by some OIB islands to calculate isochron ages of their sources, which ranged from 1-2.5 Ga. Here we follow a similar approach. However, we did not want to rely on islands yielding well-defined linear arrays in Pb isotope space. Instead, we calculate

the model ages of individual points rather than the slope of an array of data. Both approaches assume a common first stage for all samples. From this evolving reservoir a secondary model age (t_m) and U/Pb (μ_2) are calculated to produce the modern Pb isotopic composition. The parameters of our first stage evolution are given in Extended Data Item 4 together with other input values.

The Pb model age we calculate represents an event, which increased U/Pb to generate modern Pb isotopic compositions that lie to the right of the Geochron. As discussed widely (e.g. see Ref. 86), the process of subduction provides an appealing physical manifestation of this model scenario. During subduction, dehydration preferentially removes Pb from the mafic crust[87], increasing the U/Pb and Th/Pb of the deep subducted residue. Thus, we believe that the model ages relate to the time of subduction of recycled oceanic crust found in OIB sources.

Explicitly we calculate our model ages by rearranging and numerical solving the following two equations (1 and 2) for μ_2 and t_M (using parameters described in Extended Data Item 4):

Equation 1:

$$\frac{^{206}Pb}{^{204}Pb} = \frac{^{206}Pb}{^{204}Pb_{CD}} + \mu_1(e^{\lambda_{238}t} - e^{\lambda_{238}t_m}) + \mu_2(e^{\lambda_{238}t_m} - 1)$$

Equation 2:

$$\frac{^{207}Pb}{^{204}Pb} = \frac{^{207}Pb}{^{204}Pb_{CD}} + \frac{\mu_1}{137.88}(e^{\lambda_{235}t} - e^{\lambda_{235}t_m}) + \frac{\mu_2}{137.88}(e^{\lambda_{235}t_m} - 1)$$

Having obtained μ_2 and t_M a model Th/U (weight ratio) of the second stage may then be calculated accordingly by rearranging equation 3:

Equation 3:

$$\frac{^{208}Pb}{^{206}Pb} = \frac{^{208}Pb}{^{206}Pb_{CD}} + \frac{Th}{U_1} k \mu_1 (e^{\lambda_{232} t} - e^{\lambda_{232} t_m}) + \frac{Th}{U} k \mu_2 (e^{\lambda_{232} t_m} - 1)$$

Extended Data Item 3 contains the averaged calculated model Pb ages for our OIB dataset, whereas the individual model Pb ages versus measured Th/U and modeled Th/U (Pb, 2-stage) are shown in main text Fig. 3. We use Th/U (weight ratio) throughout as this is most commonly reported in the literature, although $^{232}Th/^{238}U$ (atomic ratio, kappa) is required in the calculations (albeit the difference between these two ratios is not great). The measured Th/U is potentially perturbed by melting and/or during melt migration to the surface. For this reason, we solely used samples for which U-series measurements were available which provides direct constraints on the magnitude of this process. All samples in our dataset have ^{230}Th-excesses, from 1-37% (Extended Data Item 5). This implies no more than 37% increase in Th/U during melt generation and likely less (e.g. see discussion in ref. 88). As in the case of MORB, recent melting cannot explain the trend to lower Th/U from values close to the planetary reference (3.876).

The Samoan samples are notable for having Th/U higher (4.0-5.3) than the planetary reference value. This cannot be solely a result of recent melt fractionation as these samples have minor ($^{230}Th/^{238}U$) disequilibrium (Extended Data Item 5). This high Th/U is potentially associated with lithospheric enrichment from plume-derived carbonatitic metasomatism, which can fractionate Th/U but will not influence the Pb isotopes[89]. We note that the Samoan Pb isotopes are incompatible with their high Th/U being associated with ancient fractionation, namely they have model Th/U within error of the planetary Th/U. Although the Samoan source has long been

associated with recycled continental sediments[90], if these were recycled prior to the major rise in atmospheric oxygen (as in compatible with their model age) then the Th/U of the continental material should be unfractionated[91,92] and so whether or not the enriched component is continental is not a critical issue. We also stress that the overall trend in the main text Fig. 3 is not pinned by Samoa, but includes Réunion and the enriched samples of São Miguel. For the latter, there has been a detailed discussion of why recycled sediment is not implicated in this source[28].

The apparently continuously declining Th/U of OIB and their typically higher values than MORB argues against a significant role of excess U left residual in the subducting slab lowering Th/U of OIB. Rather, we infer that the slab adds its excess U, from sea-floor alteration, to the upper mantle. As hypothesized in the main text this is likely to result from its mineralogical host becoming unstable during pro-grade metamorphism. A host such as allanite[29] would survive beyond the subduction zone, but ultimately melt to transfer U into the surrounding mantle. Thus, we infer the declining Th/U of OIB reflects the steadily decreasing Th/U of the upper mantle source, which forms crust subsequently recycled to produce further OIB. In this model, the upper mantle always has lower Th/U than previously formed OIB sources. The need for the excess U to be lost from recycled oceanic crust has also been discussed in terms of the Pb isotope systematics of OIB (e.g. see refs. 93,94).

Continued References

31 Gutjahr, M. *et al.* Reliable extraction of a deepwater trace metal isotope signal from Fe–Mn oxyhydroxide coatings of marine sediments. *Chemical Geology* **242**, 351-370 (2007).

32 Goldstein, S. J., Murrell, M. T. & Janecky, D. R. Th and U isotopic systematics of basalts from the Juan de Fuca and Gorda Ridges by mass spectrometry. *Earth and Planetary Science Letters* **96**, 134-146 (1989).

33 Bourdon, B., Goldstein, S. J., Bourles, D., Murrell, M. T. & Langmuir, C. H. Evidence from ^{10}Be and U series disequilibria on the possible contamination of mid-ocean ridge basalt glasses by sedimentary material. *Geochemistry, Geophysics, Geosystems* **1** (2000).

34 Reinitz, I. & Turekian, K. K. 230Th/238U and 226Ra/230Th fractionation in young basaltic glasses from the East Pacific Rise. *Earth and Planetary Science Letters* **94**, 199-207 (1989).

35 Andersen, M. B., Vance, D., Keech, A. R., Rickli, J. & Hudson, G. Estimating U fluxes in a high-latitude, boreal post-glacial setting using U-series isotopes in soils and rivers. *Chemical Geology* **354**, 22-32 (2013).

36 Richter, S. *et al.* The isotopic composition of natural uranium samples—Measurements using the new 233U/236U double spike IRMM-3636. *International Journal of Mass Spectrometry* **269**, 145-148 (2008).

37 Andersen, M. B. *et al.* A modern framework for the interpretation of 238U/235U in studies of ancient ocean redox. *Earth and Planetary Science Letters* **400**, 184-194 (2014).

38 Hiess, J., Condon, D. J., McLean, N. & Noble, S. R. U-238/U-235 Systematics in Terrestrial Uranium-Bearing Minerals. *Science* **335**, 1610-1614 (2012).

39 Russell, W. A., Papanastassiou, D. & Tombrello, T. A. Ca isotope fractionation on the Earth and Other solar system materials. *Geochimica et Cosmochimica Acta* **42**, 1075-1090 (1978).

40 Cheng, H. *et al.* Improvements in 230Th dating, 230Th and 234U half-life values, and U–Th isotopic measurements by multi-collector inductively coupled plasma mass spectrometry. *Earth and Planetary Science Letters* **371-372**, 82-91 (2013).

41 Steele, R. C. J., Elliott, T., Coath, C. D. & Regelous, M. Confirmation of mass-independent Ni isotopic variability in iron meteorites. *Geochimica et Cosmochimica Acta* **75**, 7906-7925 (2011).

42 Stirling, C. H., Halliday, A. N. & Porcelli, D. In search of live ^{247}Cm in the early solar system. *Geochimica et Cosmochimica Acta* **69**, 1059-1071 (2005).

43 Stirling, C. H., Halliday, A. N., Potter, E.-K., Andersen, M. B. & Zanda, B. A low initial abundance of ^{247}Cm in the early solar system: Implications for r-process nucleo-synthesis. *Earth and Planetary Science Letters* **251**, 386-397 (2006).

44 Brennecka, G. A. & Wadhwa, M. Uranium isotope compositions of the basaltic angrite meteorites and the chronological implications for the early Solar System. *Proceedings of the National Academy of Sciences* **109**, 9299-9303 (2012).

45 Brennecka, G. A. *et al.* 238U/235U Variations in Meteorites: Extant ^{247}Cm and Implications for Pb-Pb Dating. *Science* **327**, 449-451, doi:10.1126/science.1180871 (2010).

46 Amelin, Y. *et al.* U–Pb chronology of the Solar System's oldest solids with variable ^{238}U/^{235}U. *Earth and Planetary Science Letters* **300**, 343-350 (2010).

47 Rocholl, A. & Jochum, K. P. Th, U and other trace-elements in carbonaceous chondrites: implications for the terrestrial and solar-system Th/U ratios. *Earth and Planetary Science Letters* **117**, 265-278 (1993).

48 Dauphas, N., Marty, B. & Reisberg, L. Molybdenum evidence for inherited planetary scale isotope heterogeneity of the protosolar nebula. *Astrophysical Journal* **565**, 640-644 (2002).

49 Trinquier, A. *et al.* Origin of nucleosynthetic isotope heterogeneity in the solar protoplanetary disk. *Science* **324**, 374-376 (2009).

50 Barrat, J. A. *et al.* The Stannern trend eucrites: Contamination of main group eucritic magmas by crustal partial melts. *Geochimica et Cosmochimica Acta* **71**, 4108-4124 (2007).

51 Morgan, J. W. & Lovering, J. F. Uranium and thorium in achondrites. *Geochimica et Cosmochimica Acta* **37**, 1697-1707 (1973).

52 Manhes, G., Allegre, C. J. & Provost, A. U-Th-Pb systematics of the eucrite "Juvinas": precise age determination and evidence for exotic lead. *Geochimica et Cosmochimica Acta* **48**, 2247-2264 (1984).

53 Zindler, A. & Hart, S. Chemical geodynamics. *Annual Review of Earth and Planetary Sciences* **14**, 493-571 (1986).

54 Hart, S. R., Hauri, E. H., Oschmann, L. A. & Whitehead, J. A. Mantle plumes and entrainment: isotopic evidence. *Science* **256**, 517-520 (1992).

55 Farley, K. A. & Neroda, E. Noble gases in the earth's mantle. *Annual Review of Earth and Planetary Sciences* **26**, 189-218 (1998).

56 Sims, K. W. W. *et al.* Chemical and isotopic constraints on the generation and transport of magma beneath the East Pacific Rise. *Geochimica et Cosmochimica Acta* **66**, 3481-3504 (2002).

57 Waters, C. L. *et al.* Recent volcanic accretion at 9° N–10° N East Pacific Rise as resolved by combined geochemical and geological observations. *Geochemistry, Geophysics, Geosystems* **14**, 2547-2574 (2013).

58 Regelous, M. *et al.* Variations in the geochemistry of magmatism on the East Pacific Rise at 10 30′ N since 800 ka. *Earth and Planetary Science Letters* **168**, 45-63 (1999).

59 Regelous, M., Niu, Y., Abouchami, W. & Castillo, P. R. Shallow origin for South Atlantic Dupal Anomaly from lower continental crust: Geochemical evidence from the Mid-Atlantic Ridge at 26 S. *Lithos* **112**, 57-72 (2009).

60 Robinson, C. J., White, R. S., Bickle, M. J. & Minshull, T. A. Restricted melting under the very slow-spreading Southwest Indian Ridge. *Geological Society, London, Special Publications* **118**, 131-141 (1996).

61 Avanzinelli, R. *et al.* Combined 238U/230Th and 235U/231Pa constraints on the transport of slab-derived material beneath the Mariana Islands. *Geochimica et Cosmochimica Acta* **92**, 308-328 (2012).

62 Alt, J. C. & Teagle, D. A. Hydrothermal alteration of upper oceanic crust formed at a fast-spreading ridge: mineral, chemical, and isotopic evidence from ODP Site 801. *Chemical Geology* **201**, 191-211 (2003).

63 Romaniello, S. J., Herrmann, A. D. & Anbar, A. D. Uranium concentrations and 238U/235U isotope ratios in modern carbonates from the Bahamas: assessing a novel paleoredox proxy. *Chemical Geology* **362**, 305-316 (2013).

64 Alt, J. C. *et al.* Subsurface structure of a submarine hydrothermal system in ocean crust formed at the East Pacific Rise, ODP/IODP Site 1256. *Geochemistry, Geophysics, Geosystems* **11** (2010).

65 Staudigel, H. Hydrothermal alteration processes in the oceanic crust. *Treatise on Geochemistry* **3**, 511-535 (2003).

66 Chen, J., Wasserburg, G., Von Damm, K. & Edmond, J. The U-Th-Pb systematics in hot springs on the East Pacific Rise at 21 N and Guaymas Basin. *Geochimica et Cosmochimica Acta* **50**, 2467-2479 (1986).

67 Mottl, M. *et al.* Warm springs discovered on 3.5 Ma oceanic crust, eastern flank of the Juan de Fuca Ridge. *Geology* **26**, 51-54 (1998).

68 Plank T. *et al.* Proceedings of the Ocean Drilling Program, Initial Reports,. *Ocean Drilling Program, College Station, TX* **185** (2000).

69 Staudigel, H., Plank, T., White, B. & Schmincke, H.-U. Geochemical fluxes during seafloor alteration of the basaltic upper oceanic crust: DSDP Sites 417 and 418. *Geophysical Monograph Series* **96**, 19-38 (1996).

70 Shiel, A. E. *et al.* No Measurable Changes in 238U/235U due to Desorption–Adsorption of U (VI) from Groundwater at the Rifle, Colorado, Integrated Field Research Challenge Site. *Environmental Science & Technology* **47**, 2535-2541 (2013).

71 Bigeleisen, J. Nuclear size and shape effects in chemical reactions. Isotope chemistry of heavy elements. *Journal of the American Chemical Society* **118**, 3676-3680 (1996).

72 Fujii, Y., Higuchi, N., Haruno, Y., Nomura, M. & Suzuki, T. Temperature dependence of isotope effects in uranium chemical exchange reactions. *Journal of Nuclear Science and Technology* **43**, 400-406 (2006).

73 Murphy, M. J., Stirling, C. H., Kaltenbach, A., Turner, S. P. & Schaefer, B. F. Fractionation of 238U/235U by reduction during low temperature uranium

mineralisation processes. *Earth and Planetary Science Letters* **388**, 306-317 (2014).

74 Brennecka, G. A., Borg, L. E., Hutcheon, I. D., Sharp, M. A. & Anbar, A. D. Natural variations in uranium isotope ratios of uranium ore concentrates: Understanding the 238U/235U fractionation mechanism. *Earth and Planetary Science Letters* **291**, 228-233 (2010).

75 Bopp IV, C. J. *et al.* Uranium 238U/235U isotope ratios as indicators of reduction: results from an in situ biostimulation experiment at Rifle, Colorado, USA. *Environmental Science & Technology* **44**, 5927-5933 (2010).

76 Romaniello, S. J., Brennecka, G. A., Anbar, A. D. & Colman, A. S. Natural Isotopic Fractionation of $^{238}U/^{235}U$ in the Water Column of the Black Sea. *Eos. Trans. AGU* **90** (2009).

77 Partin, C. A. *et al.* Large-scale fluctuations in Precambrian atmospheric and oceanic oxygen levels from the record of U in shales. *Earth and Planetary Science Letters* **369-370**, 284-293 (2013).

78 Noordmann, J. *et al.* Fractionation of $^{238}U/^{235}U$ during weathering and hydrothermal alteration, Mineralogical Magazine A1548 (2012).

79 Class, C. & Goldstein, S. L. Plume-lithosphere interactions in the ocean basins: constraints from the source mineralogy. *Earth and Planetary Science Letters* **150**, 245-260 (1997).

80 Lundstrom, C., Hoernle, K. & Gill, J. U-series disequilibria in volcanic rocks from the Canary Islands: plume versus lithsopheric melting. *Geochimica et Cosmochimica Acta* **67**, 4153-4177 (2003).

81 Elliott, T., Blichert-Toft, J., Heumann, A., Koetsier, G. & Forjaz, V. The origin of enriched mantle beneath Sao Miguel, Azores. *Geochimica et Cosmochimica Acta* **71**, 219-240 (2007).

82 Turner, S., Hawkesworth, C., Rogers, N. & King, P. U-Th isotope disequilibria and ocean island basalt generation in the Azores. *Chemical Geology* **139**, 145-164 (1997).

83 Graham, D., Lupton, J., Albarède, F. & Condomines, M. Extreme temporal homogeneity of helium-isotopes at Piton-De-La-Fournaise, Reunion Island. *Nature* **347**, 545-548 (1990).

84 Willbold, M. & Stracke, A. Trace element composition of mantle end-members: Implications for recycling of oceanic and upper and lower continental crust. *Geochemistry, Geophysics, Geosystems* **7** (2006).

85 Patterson, C. C. Age of meteorites and the Earth. *Geochimica et Cosmochimica Acta* **10**, 230-237 (1956).

86 Chauvel, C., Hofmann, A. W. & Vidal, P. HIMU-EM: the French Polynesian connection. *Earth and Planetary Science Letters* **110**, 99-119 (1992).

87 Miller, D. M., Goldstein, S. L. & Langmuir, C. H. Cerium/lead and lead isotope ratios in arc magmas and the enrichment of lead in the continents. *Nature* **368**, 514-520 (1994).

88 Elliott, T. Fractionation of U and Th during mantle melting: a reprise. *Chemical Geology* **139**, 165-183 (1997).

89 Hauri, E. H., Shimizu, N., Dieu, J. J. & Hart, S. R. Evidence for Hotspot-Related Carbonatite Metasomatism in the Oceanic Upper-Mantle. *Nature* **365**, 221-227 (1993).

90 Wright, E. & White, W. M. The origin of Samoa: new evidence from Sr, Nd, and Pb isotopes. *Earth and Planetary Science Letters* **81**, 151-162 (1987).

91 McLennan, S. M. & Taylor, S. R. Th and U in sedimentary rocks: crustal evolution and sedimentary recycling. *Nature* **285**, 621-624 (1980).

92 Jackson, M. G. *et al.* The return of subduction continental crust in Samoan lavas. *Nature* **448**, 684-687 (2007).

93 Staudigel, H. & Hart, S. R. Alteration of basaltic glass: Mechanisms and significance for the oceanic crust-seawater budget. *Geochimica et Cosmochimica Acta* **47**, 337-350 (1983).

94 Chauvel, C., Hofmann, A. W. & Vidal, P. HIMU-EM: the French Polynesian connection. *Earth and Planetary Science Letters* **110**, 99-119 (1992).

95 Pietruszka, A. J. & Garcia, M. O. The size and shape of Kilauea Volcano's summit magma storage reservoir: a geochemical probe. *Earth and Planetary Science Letters* **167**, 311-320 (1999).

96 Sims, K. W. W. *et al.* Mechanisms of magma generation beneath Hawaii and mid-ocean ridges: Uranium/thorium and samarium/neodymium isotopic evidence. *Science* **267**, 508-512 (1995).

97 Sims, K. W. W. *et al.* Porosity of the melting zone and variations in the solid mantle upwelling rate beneath Hawaii: inferences from 238U- 230Th-226Ra and 235U-231Pa disequilibria. *Geochimica et Cosmochimica Acta* **63**, 4119-4138 (1999).

98 Kokfelt, T. F. *et al.* Combined trace element and Pb-Nd–Sr-O isotope evidence for recycled oceanic crust (upper and lower) in the Iceland mantle plume. *Journal of Petrology* **47**, 1705-1749 (2006).

99 Kokfelt, T. F., Hoernle, K. & Hauff, F. Upwelling and melting of the Iceland plume from radial variation of ^{238}U-^{230}Th disequilibria in postglacial volcanic rocks. *Earth and Planetary Science Letters* **214**, 167-186 (2003).

100 Prytulak, J. & Elliott, T. Determining melt productivity of mantle sources from ^{238}U-^{230}Th and ^{235}U–^{231}Pa disequilibria; an example from Pico Island, Azores. *Geochimica et Cosmochimica Acta* **73**, 2103-2122 (2009).

101 Prytulak, J. *et al.* Melting versus contamination effects on ^{238}U-^{230}Th-^{226}Ra and ^{235}U-^{231}Pa disequilibria in lavas from Sao Miguel, Azores. *Chemical Geology* **381**, 94-109 (2014).

102 Elliott, T. Element fractionation in the petrogenesis of ocean island basalts *Ph. D. thesis (Open University)*, pp192 (1991).

103 Marcantonio, F., Zindler, A., Elliott, T. & Staudigel, H. Os isotope systematics of La Palma, Canary Islands: evidence for recycled crust in the mantle source of HIMU ocean islands. *Earth and Planetary Science Letters* **133**, 397-410 (1995).

104 Hémond, C., Devey, C. W. & Chauvel, C. Source compositions and melting processes in the Society and Austral plumes (South Pacific Ocean): element and isotope (Sr, Nd, Pb, Th) geochemistry. *Chemical Geology* **115**, 7-45 (1994).

105 Sims, K. W. W. & Hart, S. R. Comparison of Th, Sr, Nd and Pb isotopes in oceanic basalts: implications for mantle heterogeneity and magma genesis. *Earth and Planetary Science Letters* **245**, 743-761 (2006).

106 Bosch, D. *et al.* Pb, Hf and Nd isotope compositions of the two Réunion volcanoes (Indian Ocean): A tale of two small-scale mantle "blobs"? *Earth and Planetary Science Letters* **265**, 748-765 (2008).

107 Sigmarsson, O., Condomines, M. & Bachèlery, P. Magma residence time beneath the Piton de la Fournaise Volcano, Reunion Island, from U-series disequilibria. *Earth and Planetary Science Letters* **234**, 223-234 (2005).

Extended Data Item 1 | $\delta^{238}U$ reproducibility of standards. Repeated $\delta^{238}U$ measurements of a range of standards with different matrixes (CZ-1 uraninite, BHVO-2/LP 45 E basalts, seawater) are shown. All have external reproducibility (2 standard deviation, grey shaded area) better than ±0.30‰, a similar range as the internal measurements uncertainty (2 standard error) for individual samples (see methods for further discussion). The different symbols refer to the different measurement set-up (see Supplementary Data Table 4 for details).

Extended Data Item 2 | U-Th geochemistry of analysed meteorites. a) $\delta^{238}U$ vs. U concentration for ordinary chondrites (black diamonds; "finds", red diamonds; "falls"); b) $d^{238}U$ vs. ($^{234}U/^{238}U$) for ordinary chondrites (symbols as in a) and eucrites (blue circles); c) $d^{238}U$ vs. Th/U for the same samples as above; d) A 'Caltech plot' of the $d^{238}U$ of individual meteorite samples and averages based on (1) the two only meteorites with ($^{234}U/^{238}U$) within error of secular equilibrium ("Mean (Z+J)") and (2) of all the analysed meteorites ("Mean all").

Extended Data Item 3 | Literature compilation of Pb, U and Th in Ocean Island Basalts

Extended Data Item 4 | Input parameters for calculating Pb model ages

Extended Data Items 5 | U-Th isotope systematics in the OIB used for Pb age modeling. Symbol colours are as in the main text Figure 3: (1) Hawaii; (2) Iceland; (3) Azores I; (4) La Palma; (5) French Polynesia; (6) Samoa; (7) Sao Miguel II; (8) Reunion. References can be found in Extended Data Item 3. Note that the y-axis is activity ratios whereas the x-axis is a weight ratio. Stippled line represents secular equilibrium of ($^{230}Th/^{238}U$).

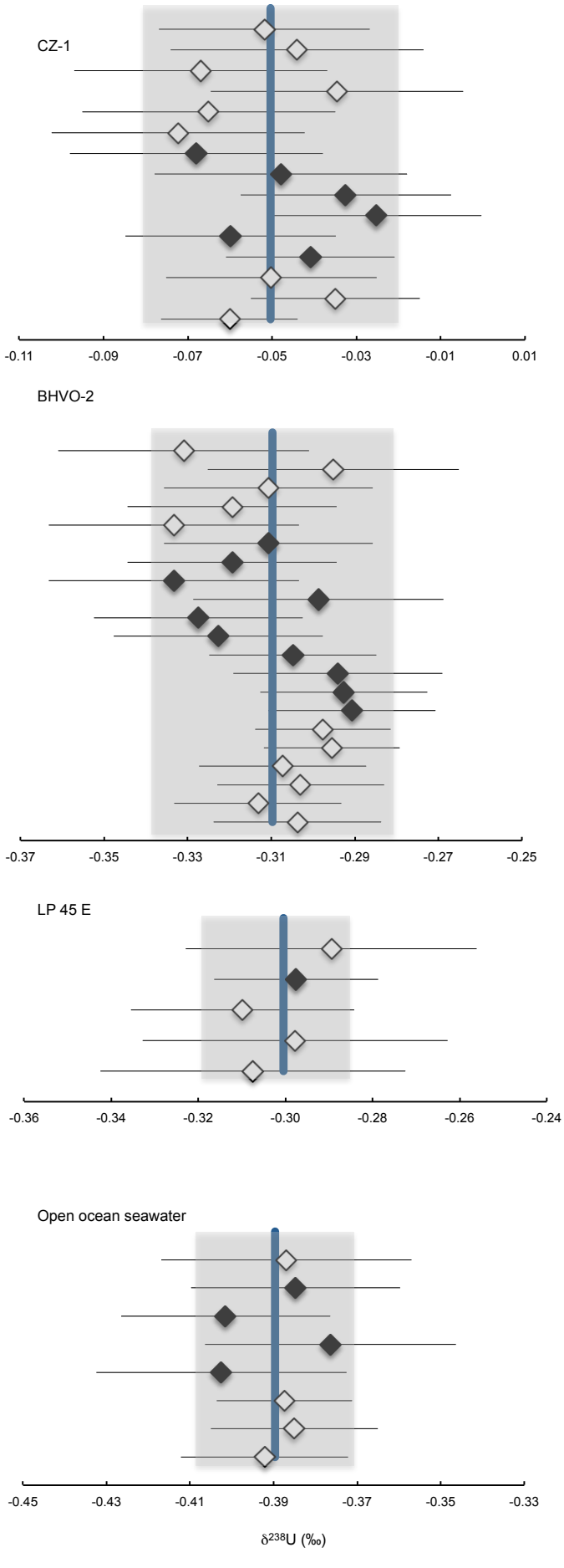
CZ-1
-0.11
-0.09
-0.07
-0.05
-0.03
-0.01
0.01
BHVO-2
-0.37
-0.35
-0.33
-0.31
-0.29
-0.27
-0.25
LP 45 E
-0.36
-0.34
-0.32
-0.30
-0.28
-0.26
-0.24
Open ocean seawater
-0.45
-0.43
-0.41
-0.39
-0.37
-0.35
-0.33
δ238U (‰)

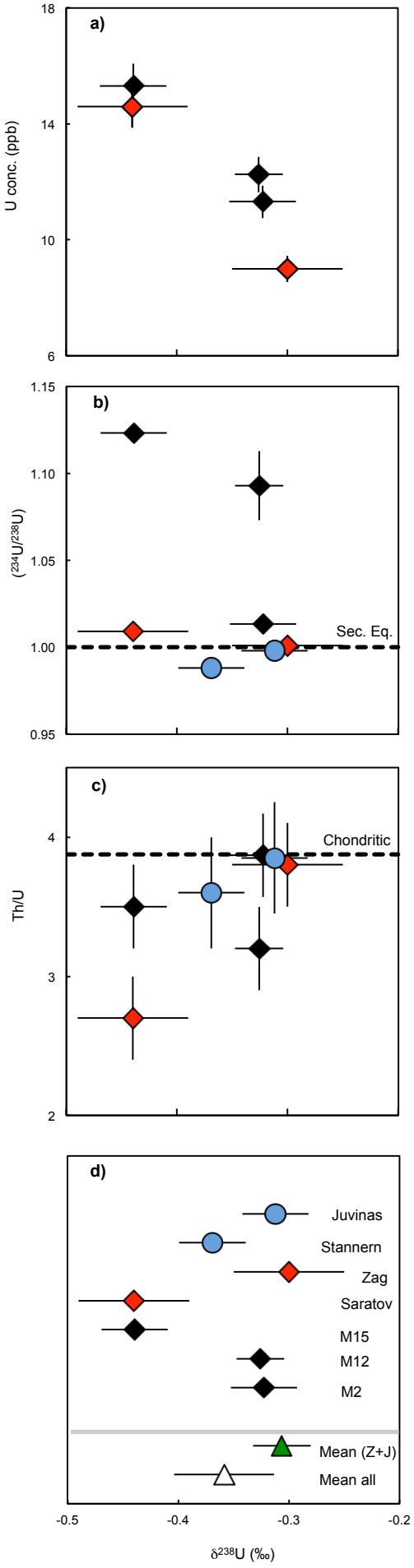
a)
U conc. (ppb)
18
14
10
6
b)
(234U/238U)
1.15
1.10
1.05
1.00
0.95
Sec. Eq.
c)
Th/U
4
3
2
Chondritic
d)
Juvinas
Stannern
Zag
Saratov
M15
M12
M2
Mean (Z+J)
Mean all
-0.5
-0.4
-0.3
-0.2
δ238U (‰)

Extended Data Item 3 | Pb, U and Th literature compilation for Ocean Island Basalts

N*	Locality	Ref. Pb	Ref. Th/U	n†	age (Ga)‡
1.	Hawaii (Kilaeua)	(95,96,97)	(95,96,97)	3	1.76
2.	Iceland	(98)	(99)	35	1.81
3.	Azores I (Sao Miguel/Pico)	(81)	(100,101)	10	1.89
4.	Canaries (La Palma)	(102,103)	(102)	8	1.92
5.	French Polynesia	(104)	(104)	11	2.12
6.	Samoa	(105)	(105)	13	2.25
7.	Azores II (Sao Miguel)	(81)	(100)	13	2.33
8.	Reunion	(106)	(107)	(average)	2.42

*Locality number used in main text Figure 3

†Number of individual data-points

‡ Average Pb model ages (t_m) for each locality, see methods

Extended Data Item 4 | Input parameters for calculating Pb model ages

Initial composition:*	
$^{206}Pb/^{204}Pb$ *(Canyon Diablo)*:	9.3066
$^{207}Pb/^{204}Pb$ *(Canyon Diablo)*:	10.293
$^{208}Pb/^{204}Pb$ *(Canyon Diablo)*:	29.475
μ_1 (1. Stage $^{238}U/^{204}Pb$):	7.85
Th/U_1 (1. Stage):	3.876
t (time ago, Ga):	4.57
$^{238}U/^{235}U$:	137.88†
k	1.03326‡
Decay constants (y^{-1}):	
λ_{238} (^{238}U):	1.551E-10
λ_{235} (^{235}U):	9.849E-10
λ_{232} (^{232}Th):	4.948E-11

*Radioactive element abundances and ratios are reported as present day values

†The "old consensus value" is used to be comparable with literature data

‡k is the conversion factor of Th/U weight ratios to atomic ratios of $^{232}Th/^{238}U$ (or kappa). We use Th/U (weight ratios) throughout the text for consistency with most literature

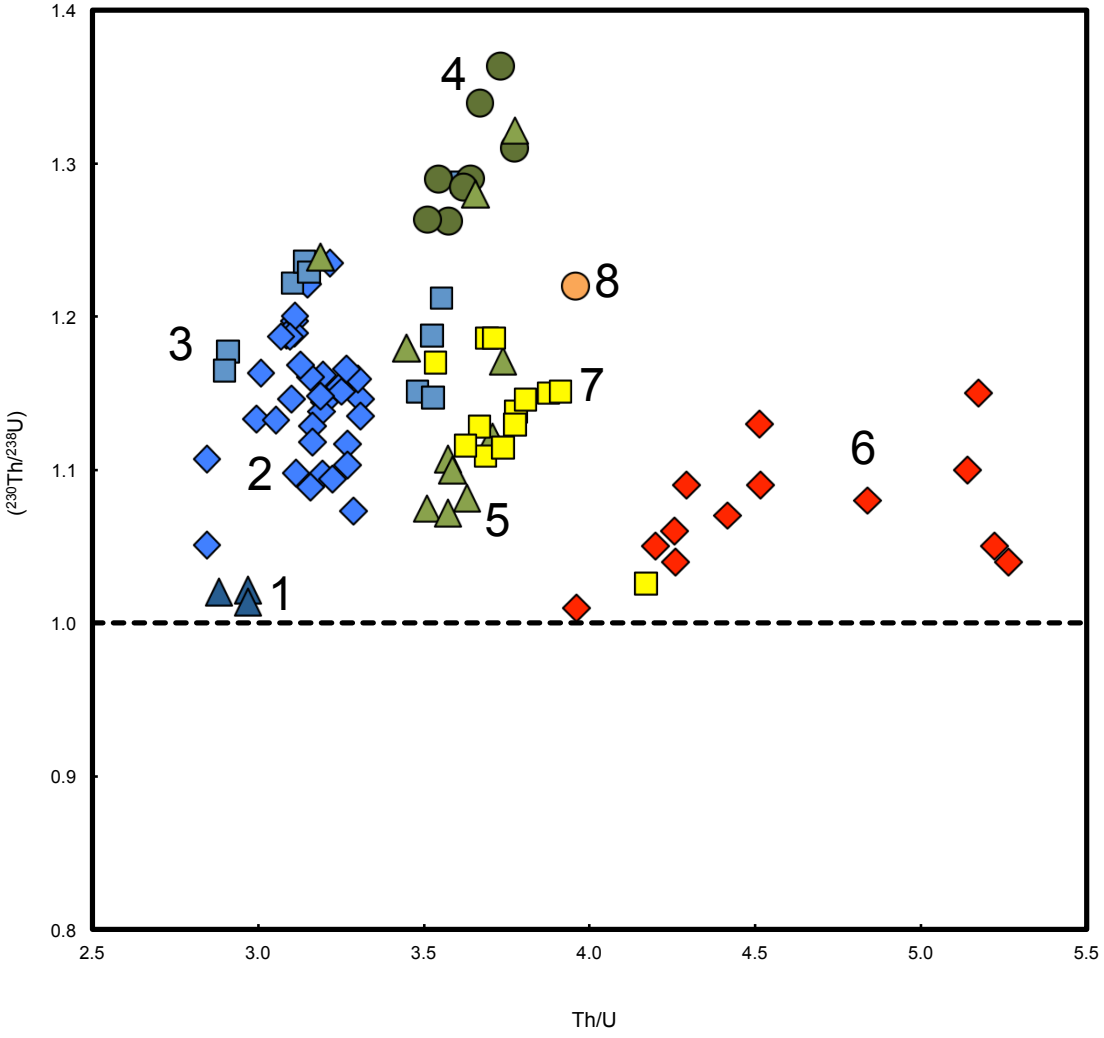
1.4
1.3
1.2
1.1
1.0
0.9
0.8
2.5
3.0
3.5
4.0
4.5
5.0
5.5
(230Th/238U)
Th/U
1
2
3
4
5
6
7
8